Contribution from Ames Laboratory and the Department of Chemistry, Iowa State University, Ames, Iowa 50011

Cobalt-Catalyzed Evolution of Molecular Hydrogen[1]

Philip Connolly and James H. Espenson*

Received April 4, 1986

Solutions of chromium(II), europium(II), or vanadium(II) chloride in hydrochloric acid evolve molecular hydrogen rapidly in the presence of trace concentrations of the cobalt(II) macrocycle $Co(dmgBF_2)_2$. The stoichiometry for Cr(II) corresponds to the net reaction $Cr^{2+} + Cl^- + H^+ = CrCl^{2+} + {}^1/_2H_2$. The kinetics are described quite adequately by the Michaelis-Menten scheme. Kinetic studies of the reaction were made during the pre-steady-state phase, during which an intensely absorbing intermediate forms, and also at longer times during the steady-state phase when the pseudo-steady-state concentration of the intermediate slowly declined as the substrate was consumed. Arguments are given in support of the intermediate being $[(H_2O)_5Cr-Cl-Co(dmgFB_2)_2]^+$. Its dissociation leads, in acidic solution, to the hydridocobalt complex $HCo(dmgBF_2)_2$, which is responsible for H_2 formation. Bromide ions, but not perchlorate, also give catalytic H_2 production, whereas iodide forms a ternary complex that does not decompose.

Introduction

Acidic solutions of chromium(II), europium(II), and vanadium(II) ions are thermodynamically unstable with respect to formation of M(III) and dihydrogen (eq 1). Nonetheless, only

$$2M_{aq}^{2+} + 2H^+ = 2M_{aq}^{3+} + H_2 \quad (1)$$

under rare circumstances do such reactions occur at a finite rate, for example, in the presence of platinized platinum.[2] To the best of our knowledge, hydrogen evolution as in eq 1 has not been reported in homogeneous, nonphotochemical processes.

In the course of certain other studies, acidic solutions of $EuCl_2$ were mixed with the Co(II) macrocycle $(H_2O)_2Co^{II}(dmgBF_2)_2$.

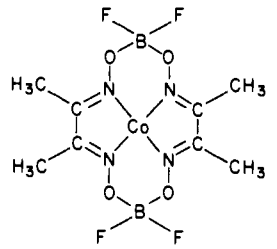

These solutions evolved copious quantities of H_2 as Eu^{2+} was converted to Eu^{3+}. This phenomenon was traced to a thermal reaction between Eu^{2+} and H^+, which is catalyzed by the Co(II) complex. Solutions of $CrCl_2$ in HCl proved to react similarly, although they too remained indefinitely unchanged without the Co(II) catalyst. Catalysis is, indeed, the correct term. A trace amount of the Co(II) complex causes the reaction to proceed until the supply of M(II) has been exhausted. Because of the novelty of this phenomenon, we decided to investigate its stoichiometry, kinetics, and mechanism.

Results

Products and Stoichiometry. When the indicated three components—MCl_2, HCl, and $Co^{II}(chel)$—are mixed, an intensification of the absorbance, especially at $\lambda > 550$ nm, occurs "immediately". Over several minutes this color fades to a stable green solution, and copious quantities of a gas are produced. The hydrogen evolved, identified by the $PdCl_2$ test,[4] was 88 ± 8% of that expected from eq 1, based on $[Cr^{2+}]_0$. (When repeated with added phenylacetylene, the yield of H_2 dropped to 16%.) Hydrogen evolution continued until no Cr^{2+} remained. The catalyst and product were separated by ion-exchange chromatography; $(H_2O)_5CrCl^{2+}$ was the only chromium species produced. Its yield was 90 ± 10% of $[Cr^{2+}]_0$. Formation of $CrCl^{2+}$ is particularly noteworthy since $Cr(H_2O)_6^{3+}$ is the thermodynamic product under the reaction conditions. The net reaction for Cr^{2+} is thus

$$Cr(H_2O)_6^{2+} + H^+ + Cl^- = (H_2O)_5CrCl^{2+} + {}^1/_2H_2(g) + H_2O \quad (2)$$

Because of the lability of europium(III) toward ligand substitution, it is meaningless to inquire whether the product from Eu^{2+} contains coordinated chloride. Hydrogen evolution does *not* occur in perchlorate solutions, however, and the cobalt-catalyzed reaction in perchlorate solutions is extremely slow. The kinetic requirement of chloride, bromide, or a similar anion for hydrogen formation suggests that the anion plays a more-than-incidental role.

The cobalt(II) complex $(H_2O)_2Co(dmgBF_2)_2$, unlike many other Co(II) complexes of N_4 macrocycles, is quite resistant to demetalation in acidic solutions over the reaction times. This characteristic is useful, because this complex remains intact where others such as $Co(dmgH)_2$[5] would not.

Proposed Reaction Sequence. Four types of measurements were made to define the kinetics. Because of that, the presentation and interpretation of the data will be clearer if a model is proposed at the outset. One credible set of reactions that can account for the data is shown in eq 3-7.

$$Cl^- + Cr^{2+} + Co^{II}(dmgBF_2)_2 \rightleftarrows [Cr-Cl-Co(dmgBF_2)_2]^+ \quad (3)$$

$$[Cr-Cl-Co(dmgFB_2)_2]^+ \rightarrow Co^{I}(dmgBF_2)_2^- + CrCl^{2+} \quad (k_4) \quad (4)$$

$$Co(dmgBF_2)_2^- + H^+ \rightarrow HCo^{III}(dmgBF_2)_2 \quad \text{(fast)} \quad (5)$$

$$2HCo(dmgBF_2)_2 \rightarrow 2Co(dmgBF_2)_2 + H_2 \quad \text{(fast)} \quad (6)$$

$$HCo(dmgBF_2)_2 + H^+ \rightarrow H_2 + Co^{III}(dmgBF_2)_2^+ \quad \text{(fast)} \quad (7a)$$

$$Co(dmgBF_2)_2^+ + Cr^{2+} + Cl^- \rightarrow CrCl^{2+} + Co(dmgBF_2)_2 \quad \text{(fast)} \quad (7b)$$

The rate-limiting steps in the sequence are the reduction of the catalyst to a transient Co(I)-containing intermediate and subsequent release of $Co^{I}(dmgBF_2)_2^-$. In light of the rate law and the $CrCl^{2+}$ product, the formation of this intermediate very likely occurs via Cl^--bridged electron transfer. Electron-transfer formation of Co(I) itself can be seen, however, to be an uphill reaction ($M^{3+/2+}$, $E°_{Cr} = -0.415$ V, $E°_{Eu} = -0.380$ V, and $E°_{V} = -0.230$ V;[5] for Co(II)/Co(I) reduction of $(H_2O)_2Co(dmgBF_2)_2$, $E°_{Co} \sim$

(1) Based in part on the Ph.D. thesis of P.C., Iowa State University, 1985.
(2) Spiro, M.; Ravno, A. *J. Chem. Soc.* **1965**, 78.
(3) It has, however, been reported that Cr^{2+} in edta solutions reduces vitamin B_{12r} to vitamin B_{12s}, which slowly reacts with water to produce B_{12r} and H_2: (a) Johnson, A. W.; Mervyn, L.; Shaw, N.; Smith, E. L. *J. Chem. Soc.* **1963**, 4146. (b) Schrauzer, G. N.; Deutsch, E.; Windgassen, R. J. *J. Am. Chem. Soc.* **1968**, *90*, 2441.
(4) Burns, D. T.; Townshend, A.; Carter, A. H. *Inorganic Reaction Chemistry*; Halsted: New York, NY, 1981; Vol. 2, p 191.
(5) (a) Adin, A.; Espenson, J. H. *Inorg. Chem.* **1972**, *11*, 686. (b) Gjerde, H. G.; Espenson, J. H. *Organometallics* **1982**, *1*, 435.
(6) The reduction of Co(II) to Co(I) macrocycles is well-known.[7,8] Reduction potentials generally lie in the range −0.5 to −1.0 V.[9-12]

0020-1669/86/1325-2684$01.50/0

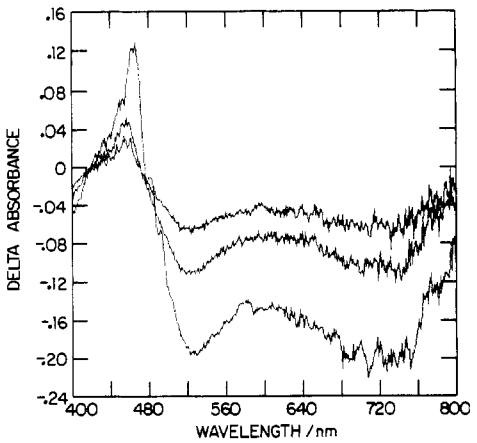

Figure 1. Difference spectra from rapid-scan stopped-flow experiments. The ordinate displays the difference between the absorbance at a given time and that at the end of the buildup phase, (i.e., after 3 s). The difference spectra define isosbestic wavelengths (420 and 475 nm) and also wavelengths (530 and roughly 755 nm) at which the intermediate has absorption maxima, since the reactants are transparent above ca. 550 nm. This particular scan shows measurements at 0.06, 0.39, and 0.72 s after mixing in an experiment with the initial concentrations 0.015 M Cr^{2+}, 0.25 M Cl^-, 0.25 M H^+, and 1.2×10^{-4} M Co(II) catalyst.

−0.43 V).[7-12] That reason, as well as evidence from the kinetic data, leads us to formulate the intermediate as $[Cr^{III}\text{–}Cl\text{–}Co^{I}(dmgBF_2)_2]^+$.

It is proposed that the Co(I) product from slow decomposition of the intermediate (eq 4) is drawn off in a subsequent fast reaction. The fate of the Co(I) is suggested on the basis of known reactions,[13-15] which include the formation of a covalent hydride (eq 5) and the ability of the hydride to evolve H_2 by both of the alternatives shown (eq 6 and 7a). (Of course, if the latter predominates, the Co(III) complex so formed must also be reduced by Cr^{2+} to yield $CrCl^{2+}$ (eq 7b).)

Analogy to Michaelis–Menten Catalysis. The reaction pattern given in eq 3–7 is analogous to the well-known Michaelis–Menten scheme for enzymatic catalysis.[16,17] This reaction scheme, eq 8–10, will be the principal model around which the presentation

$$E + S \rightleftarrows E{\cdot}S \quad (k_8, k_{-8}) \tag{8}$$

$$E{\cdot}S \rightarrow E{\cdot}P \quad (k_9) \tag{9}$$

$$E{\cdot}P \rightarrow E + P \tag{10}$$

and analysis of the data are organized. (The pair of substrates Cr^{2+} and Cl^- of eq 3 are represented as S in eq 8, and both the products as P in eq 9.) The kinetic steps in the former (eq 3, 4) are those that are written for the enzyme-catalyzed conversion (eq 8, 9). The extra reactions shown (eq 5–7) are ones that follow rapidly after the rate-limiting reactions, needed to complete the stoichiometry and regenerate the catalyst. They are known independently under similar conditions.

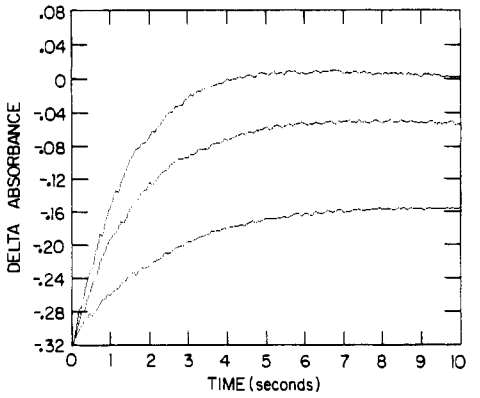

Figure 2. Absorbance–time traces from three stopped-flow kinetics experiments made during the pre-steady-state phase of the reaction. The absorbance changes were monitored at 770 nm, a maximum for the intermediate. In all three the initial concentrations were [Co(II)] = 1.1×10^{-4} M and $[Cl^-] = 0.25$ M. They had $[Cr^{2+}]_0 = 7.5 \times 10^{-3}$ M (top), 5.0×10^{-3} M (middle) and 2.5×10^{-3} M (bottom).

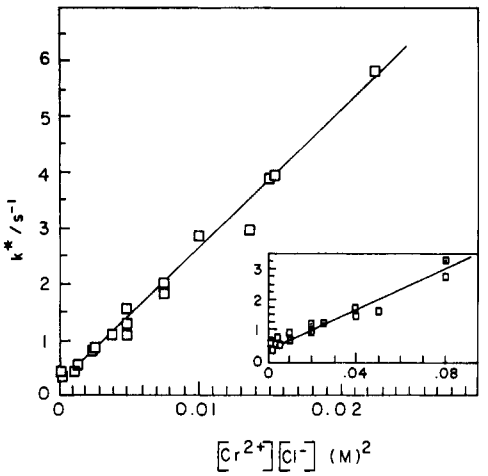

Figure 3. Rate constant k^*, characterizing the buildup of the intermediate during the pre-steady-state phase of the reaction, varying linearly with the product of the concentrations of Cr^{2+} and Cl^-, as in eq 11. Data were obtained at 25.0 °C and 1.00 M ionic strength. The inset shows analogous data for the Br^- reaction.

Experiments done by stopped-flow kinetics during the initial period of buildup of the intermediate are referred to as applying to the *pre-steady-state phase*[16,17] of the reaction. Two related but independent determinations, designated I and II in the subsequent presentation, are considered. Other experiments were done over the longer periods of time in which $[INT]_{ss}$ is decreasing and product is accumulating. They are designated as measurements made during the *steady-state phase*.[16,17] Again, two independent determinations were made, III and IV in the account that follows.

Kinetics during the Pre-Steady-State Phase: Measurements of Type I. The stopped-flow technique was used to monitor the absorbance changes on short time scales. Initially, the rapid-scan stopped-flow (RSSF) technique was used to scan rapidly and repeatedly through the appropriate spectral region so as to define the changes occurring and locate the wavelengths of interest. The results of one such experiment are shown in Figure 1.

From the guidance so obtained, the long-wavelength maximum of the intermediate was estimated as 755 nm. (Actually, a wavelength this long is defined somewhat imprecisely in this RSSF instrument, and subsequent single-wavelength determinations showed 770 nm to be a closer estimate.) The detailed kinetics of the buildup of the intermediate during the pre-steady-state phase were monitored at 770 nm. The absorbance rose smoothly to a maximum, corresponding to maximum concentration of INT, a pseudoequilibrium value.

Typical stopped-flow determinations are shown in Figure 2. The kinetic curve in each run followed a pseudo-first-order kinetic

(7) We are grateful to M. E. Brynildson for this measurement by cyclic voltammetry. The reduction potential for this complex lies at the less negative end of the range generally found[3b,8-12] for Co(II)/Co(I) macrocycles.
(8) Johnson, A. W.; Mervyn, L.; Shaw, N.; Smith, E. L. *J. Chem. Soc.* **1963**, 4146.
(9) (a) Schrauzer, G. N.; Holland, R. J. *J. Am. Chem. Soc.* **1971**, *93*, 1505. (b) Schrauzer, G. N. *Inorg. Synth.* **1968**, *11*, 61.
(10) Rillema, D. P.; Endicott, J. F. *Inorg. Chem.* **1972**, *11*, 2361.
(11) Dodd, D.; Johnson, M. D. *Organomet. Chem. Rev.* **1973**, *52*, 1.
(12) Murakami, Y. *Adv. Chem. Ser.* **1980**, *No. 191*, 179.
(13) Ryan, D. A.; Espenson, J. H. *Inorg. Chem.* **1981**, *20*, 4401.
(14) Chao, T.-H.; Espenson, J. H. *J. Am. Chem. Soc.* **1978**, *100*, 129.
(15) Evans, J.; Norton, J. J. *J. Am. Chem. Soc.* **1974**, *96*, 7577.
(16) Hiromi, K. *Kinetics of Fast Enzyme Reactions*; Halsted: New York, NY, 1979.
(17) Fromm, H. J. *Initial Rate Enzyme Kinetics*; Springer-Verlag: New York, 1975.

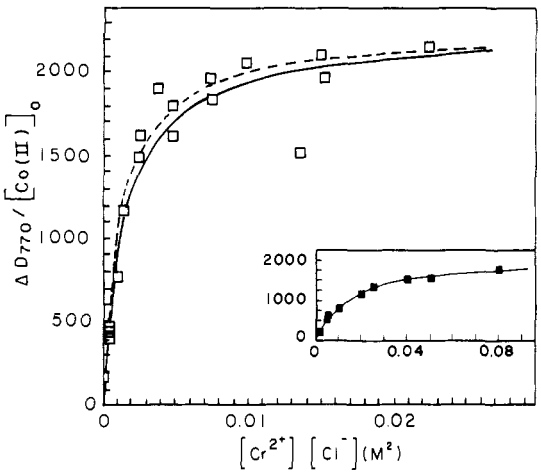

Figure 4. Plot of the absorbance change at 770 nm, normalized to the same initial [Co(II)] and to an optical path of 1 cm, vs. the product of the concentrations of Cr^{2+} and Cl^-. The data follow eq 12, derived from the mechanism in the reaction scheme. The solid line is the best fit curve, and the dashed line is based on the compromise parameters. The inset shows similar experiments for the Br^- reaction at 760 nm.

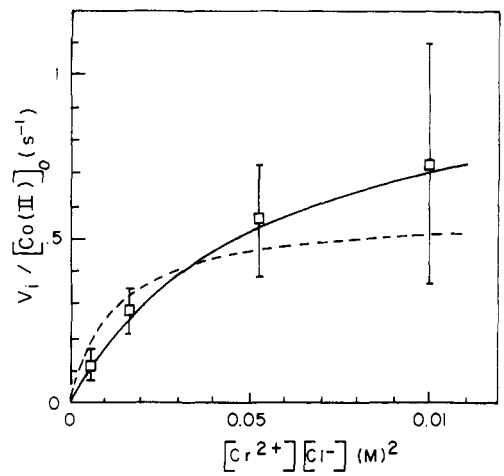

Figure 5. Initial rate of Cr^{2+} loss, determined analytically on withdrawn samples, shown as a function of $[Cr^{2+}]$. For the sake of consistency with other figures, the axes also contain $[Co(II)]_T$ and $[Cl^-]$, although they were the same in all four experiments. The solid line is the best fit curve, and the dashed line is based on the compromise parameters.

equation and yielded a rate constant designated as k^*. Values of k^* vary linearly with both $[Cr^{2+}]$ and $[Cl^-]$, as shown in Figure 3. The expression for k^* based on eq 3–7 was examined by direct mathematical analysis[18a] and by computer modeling using the program KINSIM.[19] These methods identify k^* as composite

$$k^* = (k_{-3} + k_4) + k_3[Cr^{2+}][Cl^-] \qquad (11)$$

Absorbance Changes during the Pre-Steady-State Phase: Measurements of Type II. The extent of intermediate formation can be represented by the magnitude of the absorbance change at 770 nm (ΔD_{770}) during this phase. This utilizes a different set of values derived from the same experiments used to make the measurements given in the preceding section. Its amplitude depends on the initial concentrations of Cr^{2+} and Cl^-. After a sharp rise at low concentrations, the value saturates to a plateau. Figure 4 depicts the variation. The data take the form given by eq 12, with parameter A to be identified as the molar absorptivity of the intermediate at 770 nm, ϵ_{INT}^{770}, and B the Michaelis constant, K_m or $(k_{-3} + k_4)/k_3$.

$$\frac{\Delta D}{[Co(dmgBF_2)_2]_0} = \frac{A[Cr^{2+}][Cl^-]}{B + [Cr^{2+}][Cl^-]} \qquad (12)$$

Kinetics of Cr^{2+} Loss during the Steady-State Phase: Measurements of Type III. The concentration of Cr^{2+} was determined on withdrawn aliquots at periodic intervals. Several such experiments were done at varying $[Cr^{2+}]$, all with $[Cl^-] = 0.25$ M and $[H^+] = 0.52$ M. The analyses early in each run were used to calculate the initial reaction velocity, $V_i = -d[Cr^{2+}]/dt$.

The values of V_i vary with $[Cr^{2+}]_0$ as shown in Figure 5.[20] These data, although not highly precise, clearly display kinetics that saturate in substrate concentration, characteristic of Michaelis–Menten kinetics. The chemical reactions of eq 3–7 lead to

$$\frac{V_i}{[Co(dmgBF_2)_2]_T} = \frac{C[Cr^{2+}][Cl^-]}{D + [Cr^{2+}][Cl^-]} \qquad (13)$$

The parameters in this equation can be associated with the rate constants of eq 3–7. Parameter C is $2k_4$, assuming Co(I) is lost via eq 5 and 7. (Should eq 5 and 6 instead apply, then $C = k_4$.) Parameter D is the Michaelis constant, or $(k_{-3} + k_4)/k_3$. It is important to note that, in a catalytic reaction such as this, the kinetic situation does not reduce simply to a rapid preequilibrium (eq 3) followed by a rate-limiting step (eq 4). Rather, the reaction order with respect to substrate concentration changes from the limiting value of zero at the start (when $[Cr^{2+}][Cl^-] \gg D$) to the first (provided $[Cl^-]$ is nearly constant) near the end of the catalytic conversion. This is the situation expressed by eq 13. For that reason, one would not expect to find, and we did not find, a pseudo-first-order decrease in $[Cr^{2+}]$.

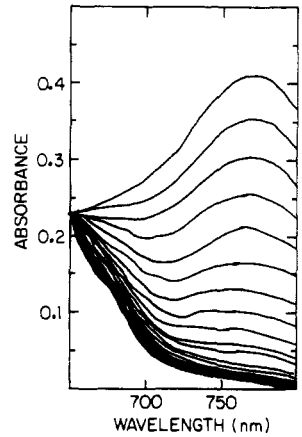

Figure 6. Intermittent scans of the visible absorption spectrum in the vicinity of the long-wavelength absorption of the reaction intermediate, showing its decay during the steady-state phase of the reaction. The spectra were recorded at 20-s intervals. Initial concentrations were 0.024 M Cr^{2+}, 0.26 M HCl, and 1.9×10^{-4} M $Co(dmgBF_2)_2$.

Kinetics of Intermediate Loss during the Steady-State Phase: Measurements of Type IV. The absorbance of the intermediate slowly fades over roughly the same period of time that $[Cr^{2+}]$ declines. Figure 6 displays one family of spectral scans taken intermittently over some 6–8 min starting immediately after the buildup phase had finished (i.e., 3 s after mixing). Copious bubbles of H_2 detracted from the precision of these measurements.

The kinetics of intermediate loss during this period are not described by a simple algebraic relation for [INT] as a function of time. It is really the concentration of the ternary intermediate that is maintained in a pseudo-steady-state value governed by the values of k_3, k_{-3}, and k_4. The expression for $[INT]_{ss}$ is implicit in eq 12. As one can see from this relation, the value of $[INT]_{ss}$ is expected to decrease with time as the substrate Cr^{2+} is consumed. This will not be a simple concentration–time relation, however, since (as seen from eq 12 and detailed in the concluding sentences

(18) (a) Reference 16, pp 222–234. (b) *Ibid.* pp 236–241.
(19) Barshop, B. A.; Wrenn, R. F.; Frieden, C. *Anal. Biochem.* **1983**, *130*, 134.
(20) Since these measurements were made at a single $[Cl^-]$, it is not really proper to represent them in eq 13 or Figure 5 as a $f([Cl^-])$. We chose to do so, however, so that these dependences (established in type I and II measurements) will be represented by analogous expressions and graphical scales.

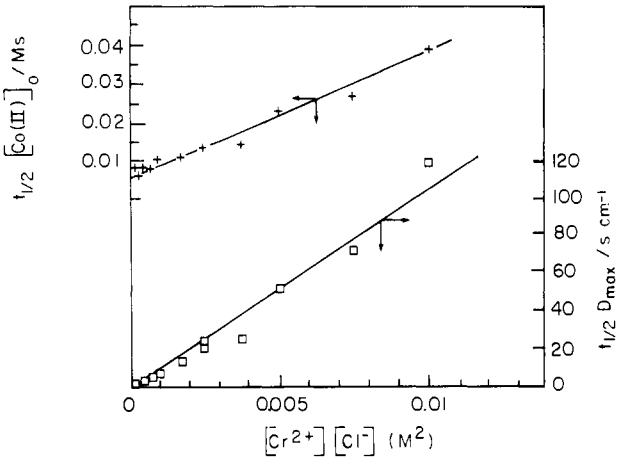

Figure 7. Plots of the data referring to the rate of absorbance decrease at 770 nm for the decay of the intermediate during the steady-state phase of the reaction. The two lines depict the linear variation as a function of substrate concentrations of (a) $t_{1/2}D_{max}$ as in eq 15 and (b) $t_{1/2}[Co(II)]_T$ as in eq 18.

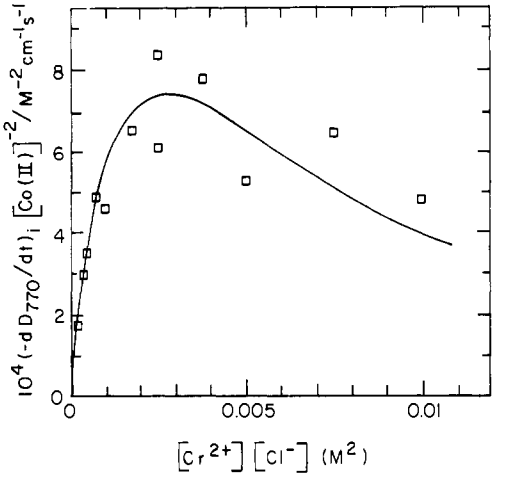

Figure 8. Plots relating the rate of absorbance loss of the intermediate to substrate concentrations. The best fit line to eq 19 is shown.

of the preceding section) the reaction order with respect to substrate increases during the course of the reaction. This situation is one that is regularly encountered in catalytic reactions; our mathematical treatment of the data follows that of Hiromi[18b] for the analogous situation in the simple Michaelis–Menten scheme. Applied to the case at hand, the maximum concentration of the intermediate (i.e., that present at the start of the steady-state phase) is given by

$$[INT]_{max} = (1/2t_{1/2}k_4[Cl^-])[Cr^{2+}][Cl^-] \quad (14)$$

Substitution of absorbance values gives a relation (eq 15) that

$$t_{1/2}D_{max} = (\epsilon_{INT}/2k_4[Cl^-])[Cr^{2+}][Cl^-] \quad (15)$$

relates measurable attributes of these experiments (i.e., D_{max} and $t_{1/2}$) to substrate concentration. The analysis of the experimental data according to eq 15 is shown in Figure 7. This graph depicts a plot of $t_{1/2}D_{max}$ vs. the substrate in concentration product. As required by eq 15, the data fall on a straight line that passes through the origin.

Hiromi's treatment of this situation,[18b] which is the one just given, can be modified further. Substitution of the usual steady-state expression for [INT] (eq 16) into eq 14 gives a relation

$$[INT]_{ss} = \frac{[Co(II)]_T[Cr^{2+}][Cl^-]}{K_m + [Cr^{2+}][Cl^-]} \quad (16)$$

$$t_{1/2}[Co(II)]_0 = (K_m/2k_4[Cl^-]) + (1/2k_4[Cl^-])[Cr^{2+}][Cl^-] \quad (17)$$

(eq 17) expressing the half-time of the decay of the intermediate to initial substrate concentration. Figure 7 also shows a plot of the data according to eq 17 which, like similar graphs,[20] uses $[Cr^{2+}][Cl^-]$ as the abscissa.

We derived[1] an expression (eq 18, 19) for $-d[INT]/dt$ during the steady-state phase of the reaction. It predicts a specific and

$$\frac{-d[INT]}{dt} = \frac{-[Co(II)]_T K_m[Cl^-](-d[Cr^{2+}]/dt)}{(K_m + [Cr^{2+}][Cl^-])^2} \quad (18)$$

$$\frac{-dD_{770}}{dt} = \frac{(2k_4\epsilon_{770}K_m[Cl^-])[Co(II)]_T{}^2[Cr^{2+}][Cl^-]}{(K_m + [Cr^{2+}][Cl^-])^3} \quad (19)$$

quite characteristic shape for the initial rate of absorbance loss as a function of substrate concentration. The data do, indeed, appear to conform to that equation (Figure 8), although the precision of the initial rate measurements was not sufficient, owing to the bubbles of H_2, for us to give them great weight. We present them here since, to the best of our knowledge, this method has not been included in treatments of Michaelis–Menten kinetics.

Table I. Kinetic Parameters[a] for H_2 Evolution Reactions

param	individual best-fit values	expt type[b]	"average" values[c]
	A: S = Cr^{2+},Cl^-		
k_3	220 ± 11 M^{-2} s^{-1}	I	220 M^{-2} s^{-1}
$k_{-3} + k_4$	0.25 ± 0.02 s^{-1}	I	0.29 s^{-1}
k_4	<0.25 s^{-1}	I	0.29 s^{-1}
	0.5 ± 0.1 s^{-1}	III	
	0.52 ± 0.04 s^{-1}	IV[d]	
	0.68 ± 0.04 s^{-1}	IV[e]	
k_{-3}	≤0.25 ± 0.02 s^{-1}	I	≪0.3 s^{-1}
K_m[f]	1.14 ± 0.10 × 10^{-3} M^2	I	1.3 × 10^{-3} M^2
	1.6 ± 0.2 × 10^{-3} M^2	II	
	5.4 ± 1.8 × 10^{-3} M^2	III	
	1.9 ± 0.2 × 10^{-3} M^2	IV	
$\epsilon_{INT}{}^{770}$	2.25 ± 0.09 × 10^3 M^{-1} cm^{-1}	II	2.25 × 10^3 M^{-1} cm^{-1}
	B: S = Cr^{2+}, Br^-		
k_3	304 ± 19 M^{-2} s^{-1}	I	
$k_{-3} + k_4$	0.43 ± 0.07 s^{-1}	I	
K_m[e]	1.4 × 10^{-3} M^2	I	
	1.52 ± 0.09 × 10^{-3} M^2	II	
$\epsilon_{INT}{}^{760}$	2.12 × 0.05 × 10^3 M^{-1} cm^{-1}	II	
	C: Eu^{2+}, Cl^-		
K_m	2 ± 1 × 10^2 M^2	II	
$\epsilon_{INT}{}^{772}$	3 ± 1 × 10^3 M^{-1} cm^{-1}	II	

[a] At 25 °C, μ = 1.00 M. [b] Derived to fit the data from each experiment separately. [c] Derived to accommodate data from all experimental types. [d] From eq 16. [e] From eq 18. [f] The final analysis is constrained to fit $K_m = (k_{-3} + k_4)/k_3$.

Numerical Treatment of the Kinetic Data. The agreement of all the data with this single model would be the best way to establish its validity. Each individual aspect does fit the predictions and requirements of the mechanism in eq 3–7. Each of the measurement types, I–IV, gives numerical parameters, some of which were independently determined two or more times. One criterion of the acceptability of the proposal is the extent to which the various parameters, thus determined, are internally consistent. Table I summarizes the numerical values. This test gives agreement with the single model that we consider as reasonable, considering the precision of the data from experiments of a given type. For example, the four independent determinations of the Michaelis constant gave values of 1.1, 1.6, 5.4, and 1.9 (×10^{-3} M^2) from experiments of types I, II, III and IV, respectively.

The precision of the different experiments varies, and thus a given parameter may be more or less accurately determined by a particular experimental type. It therefore seems a fairer test of the mechanism to ask whether a *single set* of parameters can be found to reconcile the data from all four types of experiments within the precision of the determinations. Such a set of values is also given in Table I. They were arrived at somewhat sub-

jectively by considering the character and precision of the separate measurements.

Other Variants: Br^-, I^-, Eu^{2+}, V^{2+}, and H_3O^+ Ions. Although hydrogen evolution occurs very slowly (catalyzed) or not at all (uncatalyzed) when perchlorate is the only anion in solution, the phenomenon is not unique to chloride solutions. Use of Br^- produces a similar intermediate that slowly yields H_2. A smaller data set is shown in Figures 1 and 2, with numerical values given in Table I. Iodide forms an intermediate also, but it persists without decay for a substantial time.

The formation of an intensely colored intermediate was also noted for $EuCl_2$ and VCl_2 solutions in HCl. Like the $CrCl_2$ reaction, these solutions evolved H_2 and produced MCl_3 solutions. Only these strong reducing agents are effective; $FeCl_2$ and $ZnCl_2$ solutions in HCl neither form an absorbing species when $Co(dmgBF_2)_2$ is added nor (of course) evolve hydrogen.

The data for the chromium(II) reaction during the pre-steady-state phase, ΔD and k^*, were independent of $[H_3O^+]$, 0.2–0.8 M. The rate of loss of the intermediate during the steady-state phase was decreased somewhat by decreasing $[H_3O^+]$, about 30% from 0.77 to 0.27 M. The effect was not quantified further, since the established chemistry of reactions 5–7 depends on the acidity and the rate of eq 4 as well.

Discussion

The proposed mechanism formulates the intermediate as a complex of a cobalt(I) macrocycle with $M^{III}X$. The absorption spectrum is very reminiscent of those of Co(I) macrocycles in general and of $Co(dmgBF_2)_2^-$ in particular. The latter has an absorption maximum at 625 nm (ϵ 10^4 M^{-1} cm^{-1}) in alkaline methanol. Since cobalt(I) macrocycles have very distinctive spectra, particularly regarding the intensity and location of the long-wavelength maximum, these observations support the formulation suggested. The ability of phenylacetylene to reduce sharply the extent of H_2 production is also indicative of Co(I) and the hydrido intermediate, since it is known[21] to function as an efficient trap for them.

The intermediates are not simply the Co(I) macrocycle alone, however, for the following reasons. Their spectra, although similar in all cases (V, Eu, Cr; Cl, Br), are not identical with one another and are not a perfect match with the authentic Co(I) complex by itself. The independently prepared $Co^I(dmgBF_2)_2^-$ ion evolves H_2 *instantly* when HCl is added, in contrast to the persistent character of these intermediates. The extent and rate constant for intermediate formation (k^*) proved independent of added Eu^{3+} (0.05 M) and of added $CrCl^{2+}$ (0.01 M). That shows the reverse of the first step does not contain a concentration term multiplying k_{-3}. This is also consistent with the derived result (Table I) that k_{-3} is kinetically unimportant compared to k_4.

The catalytic effect of Co(II) macrocycles on electron-transfer reactions between Cr^{2+} and Co(III) macrocycles has been noted.[10,22] The initial step proposed there is, as it is here, reduction to the Co(I) macrocycle, (eq 3). Presumably the halide ion functions here as an electron-transfer bridge, stabilizing the dinuclear intermediate. The quantitative yield of the inner-sphere $CrCl^{2+}$ complex, a kinetic but not a thermodynamic product in this system, provides definite proof of an activated complex bridged by halide. Since Eu^{2+} and Cr^{2+} probably adopt similar mechanisms, it seems reasonable to invoke the same role of chloride for Eu^{2+}, although the same proof is lacking.

The data obtained do not allow us to known which metal complex associates with halide ion first; i.e., whether eq 3 really occurs by the reaction of $CrCl^+$ with Co^{II} or of Cr^{2+} with $ClCo^{II}$. Both Cr^{2+} and $Co^{II}(dmgH)_2$ form complexes with Cl^- and Br^-; the former is quite weak, but the latter is reported to have appreciable stability (~ 1 M^{-1}).[23,24] Attempts[25] to determine the stability complex for X^- with $Co^{II}(dmgBF_2)_2$ were not successful; spectral changes proved immeasurably small, suggesting (but not proving) very weak binding between X^- and the cobalt(II) complex.

The electrode potentials cited and the stability constant for the equilibrium $Cr^{3+} + Cl^- = CrCl^{2+}$ allow calculation of the value of $K_{20} \sim 1$ M^{-2} for the equilibrium constant for the reaction

$$Cr^{2+} + Cl^- + Co(dmgBF_2)_2 = [CrClCo(dmgBF_2)_2]^+ \qquad (20)$$

Since this reaction is the sum of the reactions in eq 3 and 4, $K_{20} = k_3K_4$. The value of K_3 can be calculated from the kinetic parameters: $k_3/k_{-3} = K_3 \gg 7 \times 10^2$ M^{-2}. This in turn yields $K_4 \ll 1.4 \times 10^{-3}$ M and $k_{-4} = K_4/K_4 \gg 2 \times 10^2$ M^{-1} s^{-1}. There is little that can be done to test these values. We are, however, somewhat surprised at how large K_3 is and how small K_4 is. The binding constant between py and $Co(dmgH_2)_2^-$ is only 1.5×10^2 M^{-1},[26] smaller even than that between $CrCl^{2+}$ and $Co(dmgBF_2)_2^-$, which is given by $1/K_4 \gg 7 \times 10^2$ M^{-1}. Perhaps this large stability constant simply signals the great electron-attracting effect caused by incorporating the BF_2 groups into the structure of the macrocycle, an influence already apparent in other features such as the reduction potential.[7]

The key to hydrogen evolution is the formation of the cobalt hydride, eq 4. The hydrido complex provides a pathway[14] for H_2 formation that avoids the high-energy intermediate $H^\bullet$. Indeed, it is the thermodynamic and kinetic inaccessibility of the latter species that is the barrier to the uncatalyzed thermal reaction.

Experimental Section

The complex diaquobis[(difluoroboryl)dimethylglyoximato]cobalt(II) was prepared as described in the literature.[27] The UV–visible spectrum agreed with the reported, with maxima at 456 and 328 nm (ϵ 4.06×10^3 and 1.92×10^3 M^{-1} cm^{-1}, respectively). Solutions of $Cr(ClO_4)_2$ and $EuCl_2$ were prepared by the reduction of the corresponding MX_3 solutions with amalgamated zinc. Distilled water, purified by a Millipore-Q water system, was used.

Several types of spectrophotometric instrumentation were employed: A Durrum-Gibson stopped-flow spectrophotometer, interfaced to the OLIS 3820 data acquisition system, and a Varian Model 219 recording spectrophotometer.

Acknowledgment. We are grateful to Andreja Bakac, Herbert T. Fromm, and Douglas Kelley for helpful discussions and to B. A. Barshop and C. Frieden for providing the KINSIM program[19] used in the numerical simulations. This work was supported by the U.S. Department of Energy, Office of Basic Energy Sciences, Chemical Sciences Division, under Contract W-7405-Eng-82.

Registry No. $Co(dmgBF_2)_2$, 26220-72-4; Cr^{2+}, 22541-79-3; Eu^{2+}, 16910-54-6; V^{2+}, 15121-26-3; HCl, 7647-01-0; Br^-, 24959-67-9; ClO_4^-, 14797-73-0; I^-, 20461-54-5.

(21) Naumberg, M.; Duong, K. N. V.; Gaudemer, A. *J. Organomet. Chem.* **1970**, *25*, 231.
(22) Rillema, D. P.; Endicott, J. F. *Inorg. Chem.* **1976**, *15*, 1459.
(23) Burger, K.; Pinter, B. *J. Inorg. Nucl. Chem.* **1967**, *29*, 1717.
(24) Marov, I. N.; Panfilov, A. T.; Ivanova, E. K. *Koord. Khim.* **1976**, *2*, 948.
(25) Brynildson, M.; Espenson, J. H.; Bakac, A., unpublished observations.
(26) Schrauzer, G. N.; Deutsch, E. *J. Am. Chem. Soc.* **1969**, *91*, 3341.
(27) Bakac, A.; Espenson, J. H. *J. Am. Chem. Soc.* **1984**, *106*, 5197.